

September 1985

LRP 272/85

THEORY OF MHD WAVES

K. Appert, G.A. Collins, T. Hellsten, J. Vaclavik
and L. Villard

Paper presented at the

12th European Conference on Controlled Fusion and Plasma Physics

Budapest, Hungary, 2 - 6 September 1985

THEORY OF MHD WAVES

K. Appert, G.A. Collins, T. Hellsten*, J. Vaclavik
and L. Villard

Centre de Recherches en Physique des Plasmas,
Association Euratom-Confédération Suisse,
Ecole Polytechnique Fédérale de Lausanne, Lausanne, Switzerland

*Jet Joint Undertaking, Abingdon, Great Britain

ABSTRACT

This paper reviews recent developments in the theory of MHD waves in connection with radio-frequency heating in the Alfvén Wave and Ion Cyclotron Ranges of Frequencies (AWRF, ICRF). The account is personal and focuses on the discussion of full wave solutions and the oscillation spectra in bounded, generally inhomogeneous, plasmas. Original results are presented concerning forced ICRF oscillations in a current-carrying torus. The effects on the wave structures of the equilibrium current, the size of the device, the minority concentration and the phenomenological damping are investigated. The resonant surfaces coincide with the magnetic surfaces as in the AWRF. The poloidal extension of the resonance is small in cases where a WKB approach is permitted so that there is no conflict between full wave solutions and the WKB method.

KEYWORDS

Alfvén waves; magnetoacoustic waves; MHD waves; excitation of waves; resonance absorption; ion cyclotron heating; Alfvén wave heating; cylindrical geometry; toroidal geometry; review.

INTRODUCTION

The last decade has seen an impressive development of linear ideal MHD stability theory (Goedbloed, 1983; Gruber and Rappaz, 1985). This development has culminated in the prediction of β -limits for tokamaks (Troyon and co-workers, 1984) which are now being verified experimentally (IAEA, 1985). During the same time the linear theory of stable MHD waves has been advanced, particularly in connection with radio-frequency (r.f.) heating and with astro- and geophysics (for reviews see Appert, Vaclavik and Villard, 1984; Hasegawa and Uberoi, 1982; Roberts, 1984). In the present survey we concentrate on a few basic points concerning the role of MHD waves in r.f. heating and some new results on ICRF wave structures in toroidal plasmas. The survey is not restricted to the ideal MHD theory of the waves in question but includes material from resistive MHD, cold and some hot plasma theory.

In order to avoid any possible confusion let us start by clarifying the terminology. By MHD waves we mean the fast and slow magnetosonic waves and the Alfvén wave. These are the terms used by the MHD community. The r.f. community ignores the slow magnetosonic wave - with good reasons by the way - and calls the Alfvén wave the "slow wave" or specifies it as "shear" or "incompressible". The fast magnetosonic wave is named "fast wave" or "compressible Alfvén wave". It can, however, be misleading to characterise the Alfvén wave by the term "incompressible" because only in some simple plasma models (e.g. ideal MHD in a homogeneous plasma) does the wave motion not compress the plasma at all. We prefer therefore the MHD terminology which does not imply this property.

The MHD waves are characterised by a vanishing or a very small wave electric field component along the equilibrium magnetic field. The wave branches in question exhibit this property for frequencies much smaller than the lower hybrid frequency. We restrict ourselves to the frequency domain $\omega \lesssim \omega_{ci}$ where ω_{ci} denotes the cyclotron frequency (or the highest cyclotron frequency in a mixture). The phase velocities ω/k of the MHD waves are of the order of the Alfvén velocity c_A and hence in a one-species plasma the wavelength satisfies the relation

$$\lambda[\text{cm}] > 14 \left(\frac{\mu}{Zn_e [10^{14} \text{ cm}^{-3}]} \right)^{1/2} \quad (1)$$

where $\mu = m_i/m_p$ is the ion mass expressed in units of proton mass, Z is the charge state and n_e is the electron density. From eq. (1) it is obvious that only in large tokamaks like JET can the wavelength be much smaller than the typical radial extension of the plasma. Consequently, the often used WKB approximation is of limited value for the MHD waves in most of the existing devices. It is more appropriate to search for global solutions (oscillation modes) of the plasma cavity in question. This can either be done by determining the eigenmodes in a given cavity or by exciting it by an external antenna. Many interesting situations have been investigated since the late fifties. It is, however, difficult to do justice to this early work. We should just be reminded that modern work on MHD waves is very likely to be old material in a new context. This is particularly true for the part of this survey where we present the simple basic ideas.

The paper is structured as follows: First, we present the linear wave equation as obtained from a cold plasma model where the geometry of the magnetic field lines due to an equilibrium current is taken into account. This equation then is used to discuss the spectrum of eigenoscillations of a plasma cylinder. In the same chapter resistive and other non-ideal effects on the spectrum are briefly touched upon. In the last chapter forced oscillations, in contrast to eigenoscillations, are discussed. Certain findings concerning cylindrical plasmas are recalled and new results obtained for a full axisymmetric geometry are presented.

BASIC WAVE EQUATIONS

Ideal MHD

For the sake of its title the present survey should start with the ideal MHD theory of the MHD waves. This is, unfortunately, not possible for space reasons and the reader is referred to the original literature (Appert and co-workers, 1974, 1982a, 1982b, 1982c; Chance and co-workers, 1977; Hasegawa and Chen, 1974; Tataronis and Grossmann, 1973).

In trying to explain experimental results (de Chambrier and co-workers, 1982) concerning MHD waves in the AWRF we have found (Appert and Vaclavik, 1983a) that the waves in a low- β tokamak should rather be described by finite-frequency cold-plasma theory (Grekov, Stepanov and Tataronis, 1981) than by ideal MHD. Abandoning ideal MHD means, in particular, losing the slow magnetosonic wave and, in general, losing the possibility of treating finite- β effects on the equilibrium and the wave propagation. Since the slow magnetosonic wave has a phase velocity of the order of the ion-sound velocity it should, in a typical equithermal collisionless tokamak plasma, be heavily ion Landau damped and its loss from the theory is therefore not serious. Comparing numerical results obtained with exact and approximate MHD equations (Appert, Balet and Vaclavik, 1982a) we were unable to find important pressure terms, at least for sufficiently large frequencies. Only for waves at very low frequency with a dispersion relation near to MHD instabilities, a situation presently contemplated by Elfimov and co-workers (1984, 1985), should the finite- β effects be considered. We refrain from presenting the MHD wave equations for the additional reason that their differential structure is identical to that of the cold-plasma wave equations.

Cold Current-Carrying Plasma

Axisymmetric force-free equilibrium. For a single ion species plasma the wave equation to be presented here can be obtained from the ideal MHD equations (Kadomtsev, 1966) under the assumption of zero pressure and with the Hall current added to Ohm's law (Appert and Vaclavik, 1983a). For a multispecies plasma one starts with the equation of motion for the species in question, assumes massless electrons and derives the same equations (Appert, Vaclavik and Villard, 1983b). In contrast to a standard derivation (Stix, 1962) we allow for curved magnetic field lines due to an axial equilibrium current $\text{rot}\vec{B}_0$ where \vec{B}_0 denotes the equilibrium magnetic field. Consistent with the assumption of low β we consider an axisymmetric force-free equilibrium $\vec{B}_0 \times \text{rot}\vec{B}_0 = 0$. In a local coordinate system ("magnetic coordinates") with \vec{e}_n , $\vec{e}_\Lambda = \vec{e}_\parallel \times \vec{e}_n$, $\vec{e}_\parallel = \vec{B}_0/B_0$ (where \vec{e}_n denotes the normal to

the magnetic surface) and with $c/c_A \gg 1$ we find (Appert, Vaclavik and Villard, 1984a; Villard and co-workers, 1985) for the two non-vanishing components of the wave electric field E_n and E_Λ ,

$$\text{rot rot } \vec{E} - \frac{\omega^2}{c^2} \vec{\epsilon} \cdot \vec{E} = 0, \quad (2)$$

where $\vec{\epsilon}$ is an operator,

$$\frac{\omega^2}{c^2} \vec{\epsilon} = \frac{\omega^2}{c^2} \begin{pmatrix} \epsilon_{nn} & \epsilon_{n\Lambda} \\ -\epsilon_{n\Lambda} & \epsilon_{nn} \end{pmatrix} + \frac{\vec{B}_O \cdot \text{rot} \vec{B}_O}{B_O^2} \begin{pmatrix} \text{rot}_n \vec{e}_n & \text{rot}_n \vec{e}_\Lambda \\ \text{rot}_\Lambda \vec{e}_n & \text{rot}_\Lambda \vec{e}_\Lambda \end{pmatrix}, \quad (3)$$

and the rot operators act to the right on \vec{e}_n , \vec{e}_Λ and \vec{E} .

The first term of $\vec{\epsilon}$ is given by the usual expressions

$$\begin{aligned} (\omega^2/c^2) \epsilon_{nn} &= (\omega^2/c_A^2) \sum_i f_i / (1 - \omega^2/\omega_{ci}^2) \\ (\omega^2/c^2) \epsilon_{n\Lambda} &= (\omega^2/c_A^2) \sum_i (f_i \omega / \omega_{ci}) / (1 - \omega^2/\omega_{ci}^2). \end{aligned} \quad (4)$$

Here $f_i = n_{i0} m_i / \sum n_{i0} m_i$ and the sum extends over all ion species of mass m_i and equilibrium density n_{i0} . The Alfvén velocity is defined by $c_A^2 = B_O^2 / (4\pi \sum n_{i0} m_i)$. The time dependence of the wave field has been assumed to be $\exp(-i\omega t)$.

Equation (2) describes MHD waves in both the Alfvén Wave and the Ion-Cyclotron Range of Frequencies. For almost all the AWRF applications it is sufficient to use eq. (2) in cylinder geometry. ICRF, on the other hand, is dominated by toroidal effects. Realising that eq. (2) does not change its differential structure when the MHD limit $\omega/\omega_{ci} \rightarrow 0$ is taken one can hope to use numerical methods and computer code modules developed for MHD stability (Gruber and Rappaz, 1985) and MHD r.f. calculations (Appert and co-workers, 1982b). Using a currentless equilibrium (Itoh and co-workers, 1984) have obtained the first ICRF relevant results. Many additional computer codes are actually in

development (Colestock, 1985; Edery and co-workers, 1985; Jaeger and co-workers, 1985; Phillips and Todd, 1985, Villard and co-workers, 1985) and interesting results can be expected in the near future. Some preliminary results obtained with our own code (Villard and co-workers, 1985) will be presented in the last chapter of this survey.

We refrain from exhibiting the explicit form of eq. (2) in toroidal magnetic coordinates. As is usual in toroidal coordinates the expressions are long and not too transparent for non-specialists. The reader is referred to Villard and co-workers (1985). In cylindrical geometry, on the other hand, the equation assumes a simple transparent form which is worthwhile considering.

Cylindrical equilibrium. For what we intend to demonstrate it is sufficient to work to first order in $B_{O\theta}/B_O$ where θ and z are the poloidal and the axial coordinates respectively. Taking the space dependence as $\exp[i(m\theta + kz)]$, defining $k_{\parallel}B_O = (m/r)B_{O\theta} + kB_{Oz}$ and $k_{\perp}B_O = (m/r)B_{Oz} - kB_{O\theta}$ and eliminating E_r in favour of the wave magnetic field component B_{\parallel} we find (Appert and Vaclavik, 1983a)

$$A \frac{1}{r} \frac{d}{dr} (rE_{\perp}) = k_{\perp}GE_{\perp} + (A - k_{\perp}^2) i \frac{\omega}{c} B_{\parallel} \quad (5)$$

$$A \frac{d}{dr} (i \frac{\omega}{c} B_{\parallel}) = (G^2 - A^2)E_{\perp} - k_{\perp}G i \frac{\omega}{c} B_{\parallel} \quad (6)$$

Here $A = (\omega^2/c^2)\epsilon_{nn} - k_{\parallel}^2$ and $G = (\omega^2/c^2)\epsilon_{n\Lambda} - 2k_{\parallel}(B_{O\theta}/rB_O)$. The eqs. (5) and (6) have exactly the same differential structure as the ideal MHD wave equations (Appert, Gruber and Vaclavik, 1974) for the radial displacement ξ_r and the total perturbed pressure $P = \vec{B} \cdot \vec{B}_O / 4\pi + p$ where p denotes the perturbed kinetic pressure. The variables E_{\perp} and B_{\parallel} can indeed be identified with ξ_r and P provided one takes the limits $p = 0$ in MHD and $\omega/\omega_{ci} = 0$ in the cold plasma model, respectively. In a multi-species plasma with $\omega/\omega_{ci} \neq 0$ the displacement ξ cannot be defined and the wave motion must be described by the electromagnetic field as we have done in eqs. (2), (5) and (6). Note that working to higher orders in $B_{O\theta}/B_O$ does not change the differential

structure of eqs. (5) and (6) (Cramer and Donnelly, 1984). Note also that the variables of eqs. (5) and (6), E_{Λ} and B_{\parallel} , constitute the radial component of the Poynting vector which is, in the context of r.f. heating, the relevant component.

As in the corresponding MHD equations eqs. (5) and (6) are singular at radial points r_0 where $A(r_0) = 0$; and as in MHD these singularities are, apart from that at $r = 0$, the only singularities of the equations (Appert, Gruber and Vaclavik, 1974; Karney, Perkins and Sun, 1979). The last fact is not obvious from the corresponding second order equation,

$$\frac{d}{dr} \frac{A}{A-k_{\Lambda}^2} \frac{1}{r} \frac{d}{dr} (rE_{\Lambda}) + \left[\frac{A}{r} - \frac{G^2}{r(A-k_{\Lambda}^2)} - \left\{ \frac{d}{dr} \left(\frac{k G}{r(A-k_{\Lambda}^2)} \right) \right\} \right] rE_{\Lambda} = 0, \quad (7)$$

whose form has indeed made Stix and Swanson (1983) believe that $A - k_{\Lambda}^2 = 0$ would also lead to a singularity.

If, inconsistently with the assumption of low β and $B_{00} \ll B_0$, B_0 varied with radius it would appear that $\omega_{ci}(r) = \omega$ could also lead to a singularity. All six coefficients in eqs. (5) and (6) diverge, however, at the same rate $\sim 1/(\omega - \omega_{ci})$ and we conclude that at the radius where $\omega = \omega_{ci}$ the wave must satisfy a condition on polarisation: $d(rE_{\Lambda})/dr = rk_{\Lambda}E_{\Lambda} + i(\omega/c)rB_{\parallel}$. The same can be concluded in toroidal geometry where ω_{ci} varies spatially as $\sim 1/r$.

SPECTRUM OF EIGENOSCILLATIONS

It is most informative to study the spectrum of possible eigenoscillations in the frequency range of the MHD waves. First of all, the connection can be made with the abundant MHD literature on spectra. Secondly, a plasma column must necessarily be excited with a frequency near to a natural oscillation frequency if the antenna-plasma coupling is to be high. A good understanding can be achieved by the investigation of some very simple model cases.

Cold Plasma Model

Global oscillations. In a homogeneous currentless plasma cylinder the wave equation for B_{\parallel} is a Bessel equation with the radial wavenumber $K^2 = (A^2 - G^2)/A$. Satisfying boundary conditions of whatever type at the plasma radius $r = a$ leads to a sequence of eigensolutions $J_m(K_{\lambda}r)$, $\lambda = 1, 2, \dots, \infty$, $|K_{\lambda+1}| > |K_{\lambda}|$ and $\lim |K_{\lambda}| = \infty$. For a one species plasma one then finds (Akhiezer and co-workers, 1967) the frequency spectrum

$$(\omega_{\lambda}^2/\omega_{ci}^2)^{\pm} = X_{\lambda}^2 \left[1 \pm \left\{ 1 - \frac{\kappa_{\parallel}^2 (\kappa_{\parallel}^2 + \kappa_{\lambda}^2)}{X_{\lambda}^4} \right\}^{1/2} \right],$$

$$X_{\lambda}^2 = \frac{1}{2} [\kappa_{\parallel}^2 + (1 + \kappa_{\parallel}^2) (\kappa_{\parallel}^2 + \kappa_{\lambda}^2)], \quad (8)$$

where $\kappa_{\parallel} = c_A k_{\parallel} / \omega_{ci}$ and $\kappa_{\lambda} = c_A K_{\lambda} / \omega_{ci}$. The plus sign yields the spectrum of the eigenfrequencies of the fast magnetosonic wave, the minus sign that of the Global Eigenmodes of the Alfvén Wave (GEAW). Note that for $\lambda \rightarrow \infty$, ω_{λ}^{-} tends from below towards the accumulation point at $(\omega_{\infty}^2/\omega_{ci}^2)^{-} = \kappa_{\parallel}^2 / (1 + \kappa_{\parallel}^2)$. The accumulation point ω_{∞}^{-} satisfies $A = 0$. We can estimate the width of the frequency band occupied by the GEAW using eq. (8) with a given κ_1 and calculating the relative distance $\Delta = (\omega_{\infty}^{-} - \omega_1^{-}) / \omega_{\infty}^{-}$ from the accumulation point ω_{∞}^{-} . The result is shown in Fig. 1. Assuming that $K_1 a$ is of the order of 1 we have $\kappa_1 = c_A / a \omega_{ci}$. Typical values are for TCA: $\kappa_1 \approx 0.5$, PLT: $\kappa_1 \approx 0.2$ and JET: $\kappa_1 \approx 0.05$. We expect therefore a width of the order of 10% and can anticipate that only the fundamental mode is well detached from the accumulation point.

In the MHD limit ($\omega/\omega_{ci} = 0$) and for $B_{00} = 0$ (i.e. $G = 0$) the Alfvén wave disappears from the dispersion relation (8) because $K^2 = A$ describes merely the fast wave, and the Alfvén branch is reduced to an infinitely degenerate eigenvalue satisfying $A = 0$ with an arbitrary $E_{\Lambda}(r)$ and $B_{\parallel} = 0$. This is the point which renders the physics of the

Alfvén wave so intricate and the Alfvén wave so delicate: Any small effect can influence the "zero order" ideal MHD picture and small effects can compete with each other or cooperate. A typical example of the interplay between small effects is that of the plasma gyrotropy and the equilibrium current in $G = (\omega^2/c^2)\epsilon_{n\Lambda} - 2k_{\parallel}(B_{0\theta}/B_0)$ which is, as we have seen, responsible for the existence of the GEAW. Appert and co-workers (1984b) find indeed the largest values for Δ when the parameters, in a certain range, are such as to maximise G . Recently a case has been found (Appert and colleagues, 1985a) where the combined effects of the plasma gyrotropy, the equilibrium current and the toroidal geometry were needed to produce a particular GEAW which had been observed in the TCA experiment.

The delicacy of the Alfvén wave contrasts strongly with the robustness of the fast magnetosonic wave which is hardly influenced by anything. There is, however, one peculiar eigensolution of eqs. (5) and (6) which is commonly identified with the lowest radial eigenmode of the fast magnetosonic wave - the surface wave eigenmode (Hasegawa and Chen, 1974; Tataronis, 1975) - which at very low frequency and in a plasma surrounded by an infinite vacuum has the dispersion relation $\omega = \sqrt{2c_A k_{\parallel}}$. This mode has a certain Alfvén wave like character and is strongly influenced by the plasma gyrotropy (Appert, Vaclavik and Villard, 1984b; Cramer and Donnelly, 1983).

Continuum. If we allow for diffuse profiles of density and equilibrium current the quantities A , G , k_{\parallel} and k_{Λ} are functions of radius. A frequency ω for which a singular point r_0 ($A(r_0) = 0$) of eqs. (5) and (6) exists, is said to belong to the Alfvén continuum if $\omega < \min\omega_{ci}$ or to the ion-ion hybrid continuum, if ω lies between two ion-cyclotron frequencies. The eigenfunctions associated with such a frequency exhibit a singularity of the type $\log(r - r_0)$ and must be understood in the distributional sense. They add up to physically meaningful quantities provided causality is ensured (Barston, 1964; Sedlacek, 1971).

The continuum and the local eigenfunctions can be explained by the physical fact that the "zero order" Alfvén wave does not propagate

perpendicularly to the magnetic field; there is no way of exchanging information across the field and hence there is no collective motion; there is no wave. The situation apparently changes dramatically when small effects like the plasma resistivity, finite electron mass or temperature are introduced into the models. These three effects lead to higher order differential wave equations and do not produce continuous spectra.

Resistive MHD

Lately, the MHD stability community has devoted much attention to the spectral problem in resistive MHD. In particular see Davies (1984), Dewar and Davies (1984), Kerner, Lerbinger and Steuerwald (1985a), Lortz and Spies (1984), Pao and Kerner (1985), Ryu and Grimm (1984), Storer (1983). The common result of these investigations is, at first sight, shocking: The Alfvén continuum is replaced by discrete eigenfrequencies situated on a system of curves deep in the stable part of the complex frequency plane. As the resistivity tends towards zero, the curves remain fixed and only the two endpoints of the ideal MHD continuum are approached by eigenfrequencies of the resistive problem. There is no smooth transition between the two spectra.

A part of the puzzle can be demonstrated with the aid of the simple example of a homogeneous currentless plasma slab immersed in a constant magnetic field $\vec{B}_0 = B_0 \vec{e}_z$. Using resistive MHD equations without pressure (Davies, 1984), and assuming the solution to behave like $\exp[i(k_y y + k_z z - \omega t)]$ we can derive the wave equation

$$[\omega^2 - c_A^2 k_z^2 - i\omega\tau c_A^2 \nabla^2] [\omega^2 + (1 - i\omega\tau)c_A^2 \nabla^2] B_x = 0, \quad (9)$$

where $\nabla^2 = d^2/dx^2 - k_y^2 - k_z^2$, $\tau = c^2/(c_A^2 4\pi\sigma)$ and σ is the conductivity. There are two decoupled polarisations: the Alfvén branch nullifies the left bracket whereas the fast magnetosonic branch nullifies the other. For small enough resistivity $\omega\tau \ll 1$ the fast wave dispersion relation is only weakly modified whereas that of the Alfvén branch

$$\omega^2 + i\omega\tau c_A^2 k_l^2 - k_z^2 c_A^2 = 0, \quad (10)$$

is not approximated by $\omega^2 = c_A^2 k_z^2$ for small values of τ . We have used iK_λ for d/dx as previously so that $k_\lambda^2 = K_\lambda^2 + k_y^2 + k_z^2$. In Fig. 2 we show a spectrum of the form of eq. (10), specifically the spectrum determined by

$$z^2 + 2iz(\lambda_0^2 + \lambda^2)/S - 1 = 0, \lambda = 1, 2, 3, \dots \quad (10')$$

for $\lambda_0 = 1$ and $S = 60$. On the left side ($\text{Re } z < 0$) we schematically show how the spectrum would be modified by e.g. a diffuse density profile. Evidently, as long as there is no equilibrium current both spectra have to be symmetric with respect to the imaginary axis.

The spectrum of the homogeneous plasma has many features in common with that of a general inhomogeneous plasma. The approach of the lowest eigenmodes towards the real axis obeys the same scaling $|\text{Im } z| \sim 1/S$. Similarly, the number of modes on the circular branches scales as $S^{1/2}$. The accumulation points at $z = 0$ and $z = -i\infty$ are another common feature. When S tends towards infinity, the two accumulation points serve as pools of eigenvalues which stream down (up) towards point A and then to the left and right on the quarter circles towards the ideal MHD solution (Ryu and Grimm, 1984). In the inhomogeneous case at point B the eigenvalues are distributed in unequal numbers (Kerner, Lerbinger and Steuerwald, 1985a) on the two curves connected with the endpoints of the ideal MHD continuum.

Looking at the spectra in Fig. 2 and comparing them with the corresponding ideal MHD spectra, one could be afraid that the physics describable with the two different models would not be the same. This, however, cannot be true. Within the parameter range where both models apply the resulting physics must be the same. An explicit comparison between the two models should soon be possible using the results of Kerner and Lerbinger (1985b) concerning a resistive MHD model for heating in the AWRP. Sy (1978) has indicated how the discrete spectrum of resistive MHD can behave as a continuous spectrum in an inhomogeneous plasma while Donnelly and Cramer (1984) have compared the predictions of the two models for a specific case.

Other Small Non-Ideal Effects

As far as the theory of r.f. heating is concerned, all kinds of non-ideal effects have been treated in the past. In these studies the problem has mostly been addressed from the propagation and linear-mode-conversion point of view (Erokhin and Moiseev, 1979; Stix and Swanson, 1983). The best known effect is that of the temperature which enables the existence of short-wavelength waves in the frequency range of the cold plasma continua: the kinetic Alfvén wave (Hasegawa and Chen, 1975, 1976) in the Alfvén continuum and the ion Bernstein wave (Stix, 1965) in the ion-ion hybrid continua. Recently, a few spectral studies have appeared (Connor, Tang and Taylor, 1983; Mahajan, 1984; Van Rij, Vahala and Sigmar, 1985). So far the implications for r.f. heating with MHD waves are not clear.

If we content ourselves with a homogeneous plasma and with the range of small frequencies ($\omega \ll \omega_{ci}$) and almost perpendicular propagation ($k_x^2 + k_y^2 \gg k_z^2$), we can present the influence of three different non-ideal effects (resistivity, finite electron mass and temperature) on the ideal MHD spectrum in one simple formula

$$N_z^2 - \epsilon_{xx} + \frac{\epsilon_{xx}}{\epsilon_{zz}} N^2 = 0 \quad (11)$$

where $N^2 = k^2 c^2 / \omega^2$, $k^2 = k_x^2 + k_y^2$, $N_z^2 = k_z^2 c^2 / \omega^2$ and

$$\epsilon_{xx} = \frac{c^2}{c_A^2} \left[1 - \frac{3}{4} k^2 \rho_i^2 + i \frac{v_e \omega}{\omega_{ci} \omega_{ce}} \right],$$

$$\epsilon_{zz} = 2 \frac{\omega_{pe}^2}{k_z^2 v_{the}^2} \frac{\omega + i v_e}{\omega} \Phi \left(\frac{\omega + i v_e}{|k_z| v_{the}} \right). \quad (12)$$

Here ω_{pe} , ω_{ce} , v_e and v_{the} are the electron plasma, cyclotron and collision frequencies and the thermal velocity respectively; ρ_i denotes the ion Larmor radius and $\phi(\xi) = 1 + \zeta Z(\zeta)$ where $Z(\zeta)$ is the plasma dispersion function (Book, 1978).

The solutions for ω of eq. (11) (where again $k_x = K_\lambda$) constitute the non-ideal spectrum. Although there is nothing new here (Hasegawa and Uberoi, 1982) it is instructive to take the different limits of eq. (11), experience the metamorphoses of the Alfvén wave and interpret the results from a spectral point of view. Donnelly and Clancy (1983) have numerically studied the inhomogeneous plasma form of eq. (11) under the influence of these three non-ideal effects, illustrating the appearance of the non-ideal waves at the various limits.

Assuming cold plasma ($T_e = T_i = 0$) and a sufficiently high collision frequency ($\nu_e \gg \omega$) we find eq. (10), the resistive case. If, on the contrary, we assume that $\nu_e \ll \omega$, we find the finite- m_e Alfvén wave,

$$\omega^2 = c_A^2 k_z^2 / (1 + k^2 c^2 / \omega_{pe}^2). \quad (13)$$

This wave has obviously a real spectrum with an accumulation point at $\omega = 0$. So far, resonances with eigenmodes of this wave have only been observed in numerical calculations (Ross, Chen and Mahajan, 1982) where, in a diffuse density profile, the modes appear near the plasma edge. In principle, they should be observable in a tokamak like TCA. The fact that they have not been observed seems to be an indication for anomalous dissipation near the plasma edge.

Assuming $\nu_e = 0$ and $\omega \ll |k_z| v_{the}$ yields the kinetic Alfvén wave (Hasegawa and Chen, 1975)

$$\omega^2 = k_z^2 c_A^2 \left[1 + k^2 \rho_i^2 \left\{ \frac{3}{4} + \frac{T_e}{T_i} \left(1 - i\pi^{1/2} \frac{\omega}{|k_z| v_{the}} \right) \right\} \right]. \quad (14)$$

Clearly, it is difficult to predict the structure of the spectrum for a diffuse profile when all these effects are combined and it is not sure that some physics could be extracted from such a spectral approach. It seems, anyway, that only the eigenmodes of the simple models (MHD and cold plasma with $m_e = 0$) can indisputably be observed in experiments. We therefore recommend an economical use of additional ingredients to the physics of the Alfvén wave. This statement, however, does not concern the ion Bernstein wave which owes its existence to the combined effects of strong plasma gyrotropy and temperature and which has successfully been excited and used for plasma heating (Ono and co-workers, 1984, 1985).

FORCED OSCILLATIONS

Current-Carrying Cylinder

The most obvious theoretical approach to low-frequency r.f. heating is the forced-oscillation approach where one assumes that the plasma column or torus is surrounded by a vacuum, an antenna and, eventually a conducting shell. An imposed current with a given spatial antenna structure and frequency drives oscillations in the plasma. The vacuum electromagnetic field is a result of the antenna and the plasma currents. The power emitted by the antenna $\int \vec{j} \cdot \vec{E} d^3x$ or, equivalently, the antenna loading impedance Z can then be used to probe the plasma: eigenmodes manifest themselves by resonant peaks.

Using the cold plasma model in a cylinder with a causality enforcing phenomenological damping coefficient ν , i.e. $\omega + i\nu$ instead of ω , we find resonances (Appert, Vaclavik and Villard, 1984a, 1984b) with all the global fast magnetosonic oscillations including the surface wave "eigenmode" and with a few Global Eigenmodes of the Alfvén Wave; the distance between peaks must be larger than ν . All the resonances have a height proportional to $1/\nu$ with the exception of those whose frequencies fall into a continuum.

Modes in the Alfvén continuum have a resonance height independent of ν : they are resonantly absorbed. In small tokamaks there is only one mode with this property, the surface mode, whereas in large and high-density tokamaks higher radial eigenmodes of the fast magnetosonic wave may also fall into this class. For heating purposes in the AWRF, however, only the surface mode is of importance because it loses, in a reasonable equilibrium, its energy nearer to the centre of the plasma than the higher modes. We have unfortunately no space here to enter into the detailed physics of resonance absorption and refer the reader to the outstanding text by Artsimovich and Sagdeev (1983) where the interaction of a high-frequency electromagnetic wave with an inhomogeneous plasma slab is described. Some AWRF and ICRF relevant material can be found in Appert and co-workers (1980, 1984a, 1985b).

The behaviour of eigenmodes which fall into an ion-ion hybrid continuum has not yet been studied systematically. Recent investigations are by Cotsaftis and Sy (1983) and by Lapierre (1983). Some preliminary numerical results have been obtained by Appert and co-workers (1985b) when investigating forced oscillations described by the Budden equation. Depending on parameters the eigenmodes appear as sharp resonances or are altogether removed and replaced by conditions of zero absorption.

Current-Carrying Torus

In a cylinder, the spectrum has a simple structure because m and k are good "quantum" numbers and modes of different m and k do not interact. In a torus, however, m ceases to be a good quantum number and all kinds of interactions become possible. Wave structures excited in the AWRF and in tori with circular cross-section show, however, (Appert and co-workers, 1982b) features which are easily understandable on the basis of cylindrical results. The reason is that the phase velocities of all the MHD waves are not too far from c_A and have therefore roughly a cylindrical symmetry. In the ICRF the situation is drastically different because the propagation properties are strongly influenced by the line $\omega = \omega_{ci}(r)$ which completely breaks the symmetry. The resulting mode structures are complicated and exhibit features of both the plane slab and the cylindrical geometry. Presently, such mode structures are under investigation and we hope that these studies will contribute to a better understanding of ICRF heating.

There is no space here for the presentation of the toroidal-geometry formalism. We just mention that it is analogous to that used in the AWRF by Appert and co-workers (1982b) and is described by Villard and co-workers (1985). We have developed the computer code LION (Lausanne ion cyclotron code) enabling us to solve eq. (2) in a general axisymmetric force-free equilibrium which can be either analytical or numerical. So far the code has only been used for Solov'ev equilibria which are provided as test equilibria by the ERATO code (Gruber and Rappaz, 1985). These equilibria are not force-free; we, however, do not expect the MHD wave structures in the ICRF to depend significantly on effects of the

order of β . Presently, LION runs on a CDC Cyber 855 computer and the finest spatial mesh possible consists of 80 x 57 nodes. It uses a large amount of disc storage and is for this reason not yet acceptable on a CRAY. The necessary modifications will be introduced in the near future. Presently we can obtain well converged results for small and moderately large devices only.

Effect of Current

In Figures 3 and 4 we show the influence of the equilibrium plasma current on wave structures. All the cases shown are for equilibria with circular cross-sections of minor radius a and a major radius R . In the first case, Fig. 3, we have chosen an (academic) aspect ratio of $R/a = 7.3$. The gas mixture is D/H with $f_D/f_H = 95/5$ (mass fractions!). The density profile is parabolic having a boundary value of 5% of the center value. The unrealistic q -profile (safety factor: 1 on the magnetic axis and 1.08 at the boundary) is a consequence of the Solov'ev equilibrium. The quantity $\omega_{CH}a/c_A = 3.3$, evaluated on the magnetic axis, characterises the device as small. The exciting antenna has strong poloidal currents on the high field side of the plasma. It is characterised by a toroidal wavenumber $n = 4$. The excitation frequency is $\omega = \omega_{CH}(0)$. Causality is ensured by adding $2i\delta$ to $(c_A^2/c^2)\epsilon_{nn}$, eq. (4). For Figures 3-6 we have used $\delta = 0.01$.

Most interestingly, the power deposition density, and hence the wave field, shows a resonant behaviour on particular magnetic surfaces as predicted analytically by Hellsten and Tennfors (1984). The poloidal extension of these resonances is independent of δ and has been found to scale roughly with $q^{-1/2}$. An extreme case of a very small equilibrium current is shown in Fig. 4 where q is 100 on the axis and 108 at the boundary. As the equilibrium current disappears the poloidal extension of the resonances shrinks to zero and the number of resonant surfaces seems to increase. Note also that the energy is deposited (or converted) near the line where $(\omega^2/c^2)\epsilon_{nn} - n^2/R^2 = 0$ (denoted henceforth by) as one expects from WKB arguments. The line $\omega = \omega_{ci}$ (here $i = H$) is indicated by the symbol -.-.-.

The $q^{-1/2}$ scaling can plausibly be explained by the following WKB argument. The wave structure along a resonant surface satisfies the approximate local dispersion relation $(\omega^2/c^2)\epsilon_{nn} = k_{\parallel}^2 = (n/R + k_p B_p/B_T)^2$ where B_p , B_T and k_p stand for the poloidal and the toroidal magnetic field and the poloidal wavenumber, respectively. The dispersion relation determines $Rk_p B_p/B_T = k_p r/q$. When the current changes k_p must vary with q because ϵ_{nn} remains constant. The amplitude of the WKB solution behaves as $k_p^{-1/2}$ and hence the poloidal extension as $q^{-1/2}$.

Effect of Size

As the magnetic-surface structure of the resonances cannot be obtained by the WKB method this feature should tend to disappear in larger plasmas where the WKB method is applicable. That the solution shows this tendency can be seen in Fig. 5. All the parameters are the same as for Fig. 3 except $\omega_{CHa}/c_A = 13.2$ and $\omega = \omega_{CH} = 2 \omega_{CD}$ which indicates that the device in Fig. 5 is 4 times larger than that in Figs. 3 and 4. The wavelengths consequently are 4 times shorter compared to the size of the device and hence the poloidal extension which scales as $k^{-1/2}$ should be half that in Fig. 3. This is roughly the case. We conclude that there is a smooth transition from the full wave solution to the WKB solution.

Effect of Minority Concentration in the AWRF

In Figure 6 we demonstrate how the "cylindrical" features (Fig. 6a) of the wave structures in the AWRF of a hydrogen plasma ($\omega \ll \omega_{CH}$) is destroyed by the addition of 4% (mass fraction) of tritium whose $\omega = \omega_{CT}$ line crosses the plasma. The parameters are the following: $R/a = 3.6$, $a\omega_{CH}/c_A = 4.425$, $\omega = 1.1 \omega_{CT}(0)$. The exciting antenna is a double helix with strong poloidal currents on the high and on the low-field side. It is characterised by the toroidal and the poloidal wavenumbers $n = -4$ and $m = \pm 1$. The aspect ratio is typical of TCA; the resulting q -profile extends from 1 to 1.4. Most strikingly, the even structure of the resonant surfaces in the single species plasma decays

into a complicated island structure (Fig. 6b) when a $\omega = \omega_{ci}$ line (here $i = T$) cuts the corresponding magnetic surface. The number of islands per surface seems to obey simple laws which, however, have not yet been formulated.

Effect of Phenomenological Damping

In all our previous numerical models for the AWRP we have ensured the causality by replacing ω by $\omega + i\nu$. Itoh and co-workers (1984) have resorted to the same trick for their ICRF calculations. In this frequency range, however, the $\omega + i\nu$ procedure greatly distorts the wave structures due to the fact that the $1 - (\omega + i\nu)^2 / \omega_{ci}^2$ denominators in ϵ , eq. (4), lead to large artificial ion-cyclotron absorption which acts not only on the left-hand polarised electric field as it should but also on the right-hand polarised field. Figure 7 was obtained for parameters identical to those of Fig. 6b with the exception of using $\omega + i\nu$, where $\nu/\omega = 0.005$. Here, the structure of the power deposition is entirely dominated by the false ion-cyclotron absorption. Since we are considering a resonance absorption process the total power absorbed should not depend on the phenomenological damping. We indeed find that the total powers obtained for Figs. 6b and 7 differ by only 10%. Astonishingly, we even find that the power deposition profiles averaged over magnetic surfaces are almost identical. In Figure 8 we show the profiles of the radial power flow normalized to one at the boundary for the two cases.

ACKNOWLEDGEMENTS

We thank M. Brambilla, D. Düchs, R. Gruber, J. Jacquinot, W. Kerner, K. Lerbinger, P. Lallia, T. Stringer, E. Tennfors, F. Troyon and J. Wesson for good discussions. This investigation was partly supported by the Swiss National Science Foundation.

REFERENCES

- Akhiezer, A.I., I.A. Akhiezer, R.V. Polovin, A.G. Sitenko, and K.N. Stepanov (1967). Collective Oscillations in a Plasma. M.I.T. Press, Cambridge, USA. Ch. II.
- Appert, K., R. Gruber, and J. Vaclavik (1974). Physics Fluids, 17, 1471-1472.
- Appert, K., B. Balet, R. Gruber, F. Troyon, T. Tsunematsu, and J. Vaclavik (1980). Proc. 2nd Grenoble-Varenna Int. Symp., Como. Commission of the European Communities, Vol. 2, 643-654.
- Appert, K., B. Balet, and J. Vaclavik (1982a). Physics Letters, 87A, 233-236.
- Appert, K., B. Balet, R. Gruber, F. Troyon, T. Tsunematsu, and J. Vaclavik (1982b). Nuclear Fusion, 22, 903-919.
- Appert, K., R. Gruber, F. Troyon, and J. Vaclavik (1982c). Plasma Physics, 24, 1147-1159.
- Appert, K., and J. Vaclavik (1983a). Plasma Physics, 25, 551-561.
- Appert, K., J. Vaclavik, and L. Villard (1983b). 11th Europ. Conf. on Controlled Fusion and Plasma Physics. Europhysics Conference Abstracts, Vol. 7D, Part I, pp. 305-308.
- Appert, K., J. Vaclavik, and L. Villard (1984a). Lecture Notes: An Introduction to the Theory of Alfvén Wave Heating. Lausanne Report, LRP 238/84, Centre de Recherches en Physique des Plasmas, Lausanne, Switzerland.
- Appert, K., J. Vaclavik, and L. Villard (1984b). Physics Fluids, 27, 432-437.
- Appert, K., G.A. Collins, F. Hofmann, R. Keller, A. Lietti, J.B. Lister, A. Pochelon, and L. Villard (1985a). Phys. Rev. Lett., 54, 1671-1674.
- Appert, K., T. Hellsten, J. Vaclavik, and L. Villard (1985b). Textbook finite element methods applied to linear wave propagation problems involving conversion and absorption. Paper contributed to 3rd. Europ. Workshop on Problems in Numerical Modeling of Plasmas, Varenna. To appear in Comput. Phys. Commun.
- Artsimowitsch, L.A., and R.S. Sagdejew (1983). Plasmaphysik für Physiker. Teubner, Stuttgart. Abschnitt 1.7.

- Barston, E.M. (1964). Annals of Physics, 29, 282-303.
- Book, D.L. (1978). NRL Plasma Formulary. Naval Research Laboratory, Washington, D.C.
- De Chambrier, A., A.D. Cheetham, A. Heym, F. Hofmann, B. Joye, R. Keller, A.Lietti, J.B. Lister, and A. Pochelon (1982). Plasma Physics, 24, 893-902.
- Chance, M.S., J.M. Greene, R.C. Grimm, and J.L. Johnson (1977). Nuclear Fusion, 17, 65-85.
- Colestock, P.L. (1985). Private Communication.
- Connor, J.W., W.M. Tang, and J.B. Taylor (1983). Physics Fluids, 26, 158-163.
- Cotsaftis, M. and W.N.-C. Sy (1983). Physics Letters, 93A, 193-197.
- Cramer, N.F., and I.J. Donnelly (1983). Plasma Physics, 25, 703-712.
- Cramer, N.F., and I.J. Donnelly (1984). Plasma Physics Contr. Fusion, 26, 1285-1298.
- Davies, B. (1984). Physics Letters, 100A, 144-148.
- Dewar, R.L., and B. Davies (1984). J. Plasma Physics, 32, 443-461.
- Donnelly, I.J. and N.F. Cramer (1984). Plasma Physics Cont. Fusion, 26, 769-787.
- Donnelly, I.J. and B.E. Clancy (1983). Aust. J. Phys., 36, 305-319.
- Edery, D., D.J. Gambier, H. Picq, and A. Samain (1985). A finite element approach for ICRF heating calculations in real tokamak plasmas. Paper contributed to 3rd Europ. Workshop on Problems in Numerical Modeling of Plasmas, Varenna. To appear in Comput. Phys. Commun.
- Elfimov, A.G., S.N. Lozovskij, and V.V. Dorokhov, Jr. (1984). Nuclear Fusion, 24, 609-611.
- Elfimov, A.G. (1985). Fizika Plazmy, 11, 550-557.
- Erokhin, N.S., and S.S. Moiseev (1979). In M.A. Leontovich (Ed.) Reviews of Plasma Physics, Vol. 7. Consultants Bureau, New York, 181-255.
- Goedbloed, J.P. (1983). Lecture Notes on Ideal Magnetohydrodynamics. Rijnhuizen Report 83-145, FOM-Instituut voor Plasmafysica, Rijnhuizen, Nieuwegein, Nederland.
- Grekov, D.L., K.N. Stepanov, and J.A. Tataronis (1981). Sov. J. Plasma Phys., 7, 411-417.
- Gruber, R., and J. Rappaz (1985). Finite Element Methods in Linear Ideal Magnetohydrodynamics. Springer, Berlin.
- Hasegawa, A., and L. Chen (1974). Phys. Rev. Lett., 23, 454-456.

- Hasegawa, A., and L. Chen (1975). Phys. Rev. Lett., 35, 370-373.
- Hasegawa, A., and L. Chen (1976). Physics Fluids, 19, 1924-1934.
- Hasegawa, A., and Ch. Uberoi (1982). The Alfvén Wave. Technical Information Center, U.S. Department of Energy.
- Hellsten, T., and E. Tennfors (1984). Physica Scripta, 30, 341-345.
- IAEA (1985). Plasma Physics and Controlled Fusion Research 1984, Vol. I. International Atomic Energy Agency, Vienna. Papers on ASDEX 71-85, PDX 117-130, TOSCA and CLEO 205-215 and DOUBLET III, 217-228.
- Itoh, K., S.-I. Itoh, and A. Fukuyama (1984). Nuclear Fusion, 24, 13-31.
- Jaeger, E.F., D.B. Batchelor, and H. Weitzner (1985). Full wave finite difference calculation for ICRF wave fields in tokamak and stellarator geometry. Paper contributed to 3rd Europ. Workshop on Problems in Numerical Modeling of Plasmas, Varenna. To appear in Comput. Phys. Commun.
- Kadomtsev, B.B. (1966). In M.A. Leontovich (Ed.), Reviews of Plasma Physics, Vol. 2. Consultants Bureau, New York, 153-199.
- Karney, C.F.F., F.W. Perkins, and Y.-G. Sun (1979). Phys. Rev. Lett., 42, 1621-1624.
- Kerner, W., K. Lerbinger, and J. Steuerwald (1985a). Computing complex eigenvalues of large non-hermitian matrices. To appear in Comput. Phys. Commun.
- Kerner, W. and K. Lerbinger (1985b). Alfvén wave heating in resistive MHD. Paper contributed to 3rd Europ. Workshop on Problems in Numerical Modeling of Plasmas, Vrenna. To appear in Comput. Phys. Commun.
- Lapierre, Y. (1983). J. Plasma Physics, 29, 223-241.
- Lortz, D., and G.O. Spies (1984). Physics Letters, 101A, 335-337.
- Mahajan, S.M. (1984). Physics Fluids, 27, 2238-2247.
- Ono, M., G.A. Warden, and K.L. Wong (1984). Phys. Rev. Lett., 52, 37-40.
- Ono, M. and others (1985). Phys. Rev. Lett., 54, 2339-2342.
- Pao, Y.-P., and W. Kerner (1985). Physics Fluids, 28, 287-293.
- Phillips, M.W., and A.M.M. Todd (1985). The numerical solution of ICRF fields in axisymmetric mirrors. Paper contributed to 3rd Europ. Workshop on Problems in Numerical Modeling of Plasmas, Varenna. To appear in Comput. Phys. Commun.
- Van Rij, W.I., G. Vahala, and D. Sigmar (1985). Spectral properties of the kinetic Alfvén wave in cylindrical tokamak geometry. Physics Fluids, accepted.

- Roberts, B. (1984). In T.D. Guyenne (Ed.), The Hydromagnetics of the Sun. 4th European Meeting on Solar Physics, Noordwijkerhout.
- Ross, D.W., G.L. Chen, and S.M. Mahajan (1982). Physics Fluids, 25, 652-667.
- Ryu, C.M., and R.W. Grimm (1984). J. Plasma Physics, 32, 207-237.
- Sedlacek, Z. (1971). J. Plasma Physics, 5, 239-263.
- Stix, T.H. (1962). The Theory of Plasma Waves, McGraw-Hill, New York.
- Stix, T.H. (1965). Phys. Rev. Lett., 15, 878-882.
- Stix, T.H., and D.G. Swanson (1983). In M.N. Rosenbluth and R.Z. Sagdeev (Ed.), Handbook of Plasma Physics, Vol. 2. North-Holland Publishing Company, Amsterdam, Ch. 2.4.
- Storer, R.G. (1983). Plasma Physics, 25, 1279-1282.
- Sy, W.N-C. (1978). Physics Fluids, 21, 702-704.
- Tataronis, J., and W. Grossmann (1973). Z. Physik, 261, 203-216 and 217-236.
- Tataronis, J.A. (1975). J. Plasma Physics, 13, 87-105.
- Troyon, F., R. Gruber, H. Saurenmann, S. Semenzato, and S. Succi (1984). Plasma Physics Contr. Fusion, 26, 209-215.
- Villard, L., K. Appert, R. Gruber, and J. Vaclavik (1985). Global waves in cold plasma. Invited paper to the 3rd Europ. Workshop on Problems in Numerical Modeling of Plasmas, Varenna. To appear in Computer Physics Reports.

FIGURE CAPTIONS

- Fig. 1: Relative distance Δ in frequency between a GEAW with radial wavenumber κ_1 and the accumulation point as a function of the parallel wavenumber κ_{\parallel} .
- Fig. 2: Eigenfrequency spectra typical of the resistive MHD model.
- Fig. 3: Power deposition density in a small device with large current.
- Fig. 4: Power deposition density in a small device with small current.
- Fig. 5: Power deposition density in a large device with large current.
- Fig. 6: Effect of a minority species (b) on the wave structure in the AWRP in a single species plasma (a). The power deposition density is shown.
- Fig. 7: Power deposition density obtained with $\omega + i\nu$ instead of $(c_A^2/c^2)\epsilon_{nn} + 2i\delta$ as used in Fig. 6b.
- Fig. 8: Normalised radial power flow versus the radial flux surface coordinate for the two different causality-ensuring models used in Figs. 6b and 7.

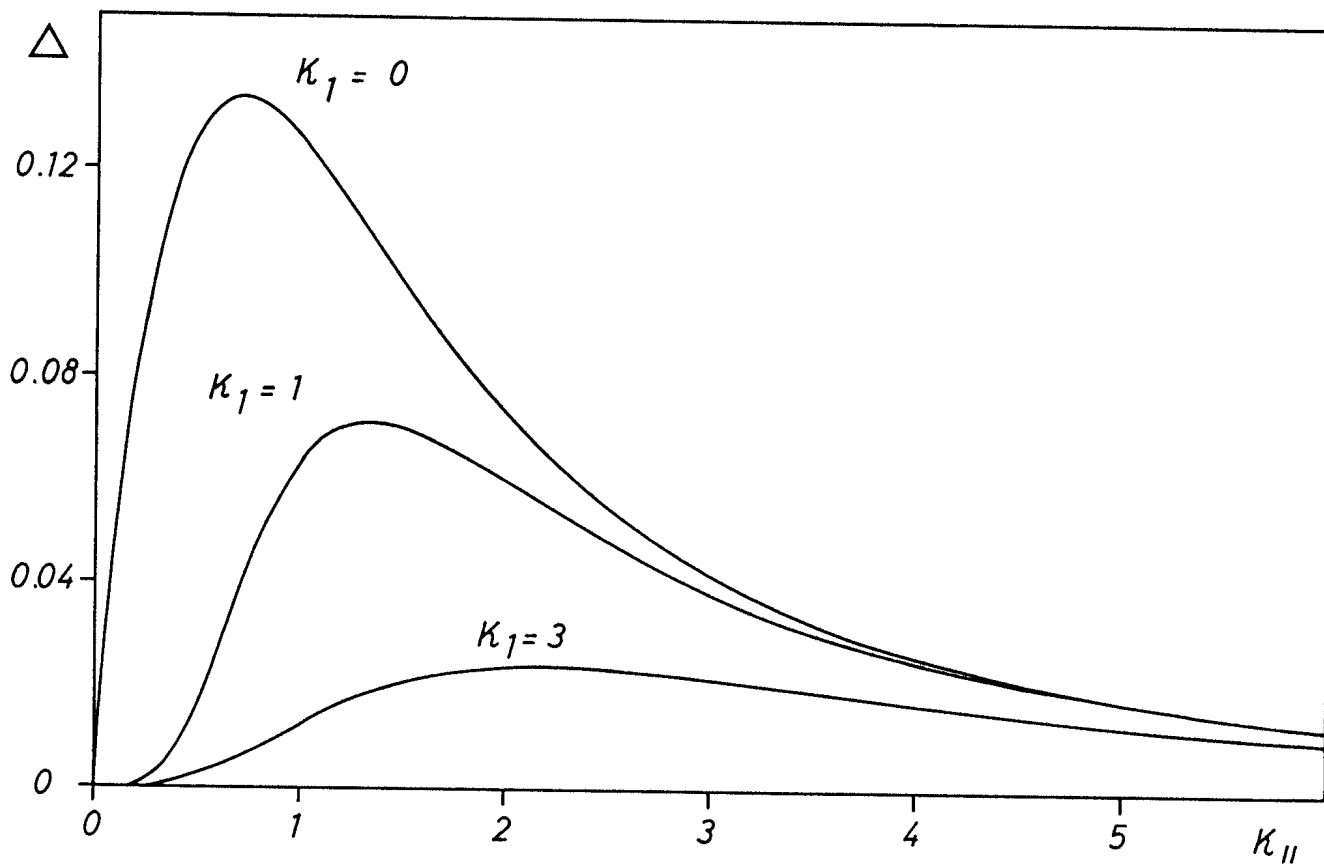


FIG. 1

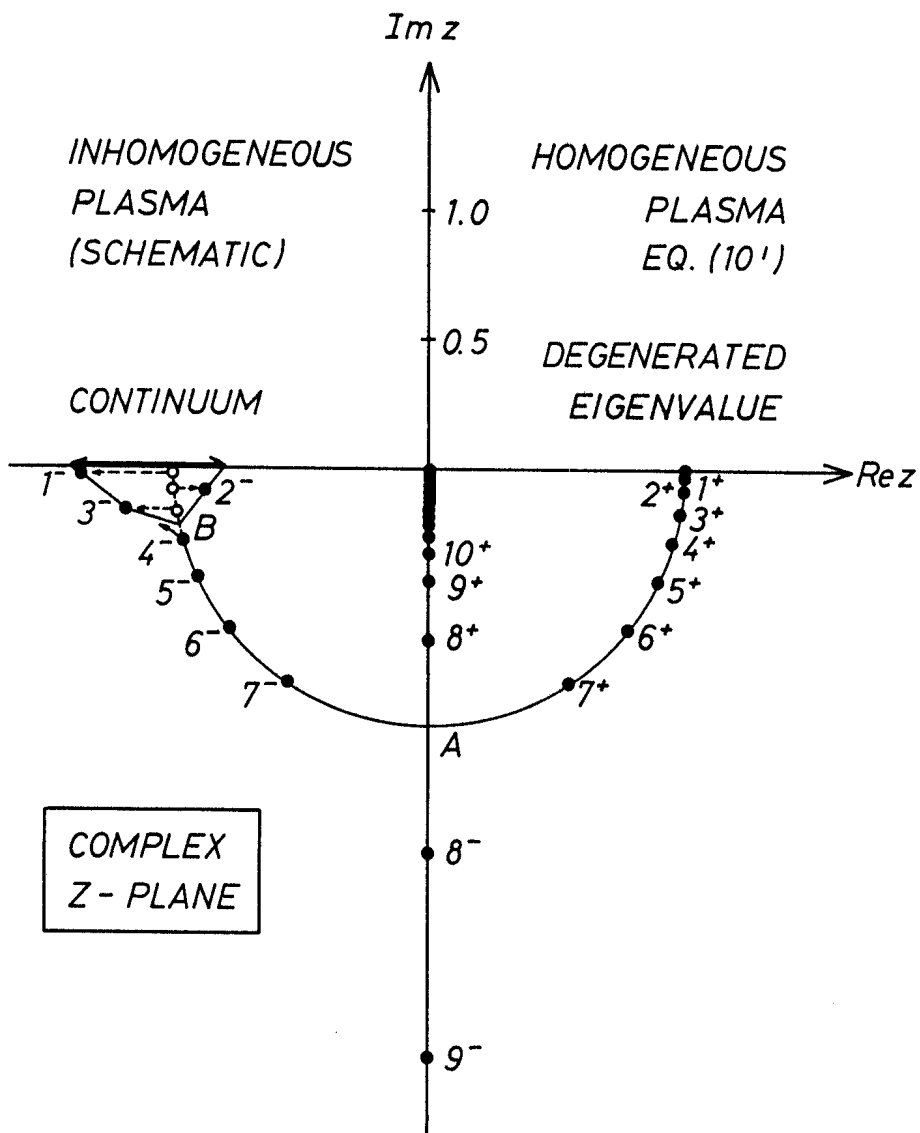
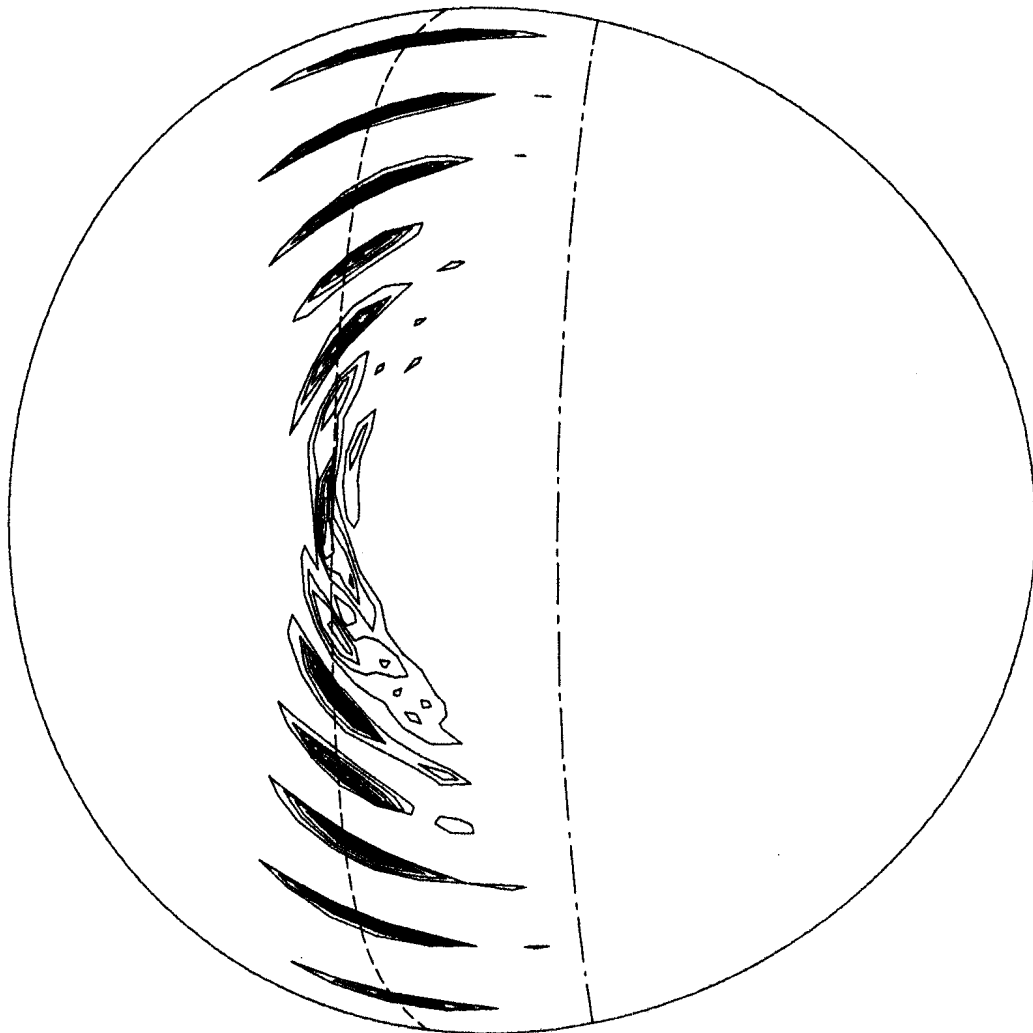
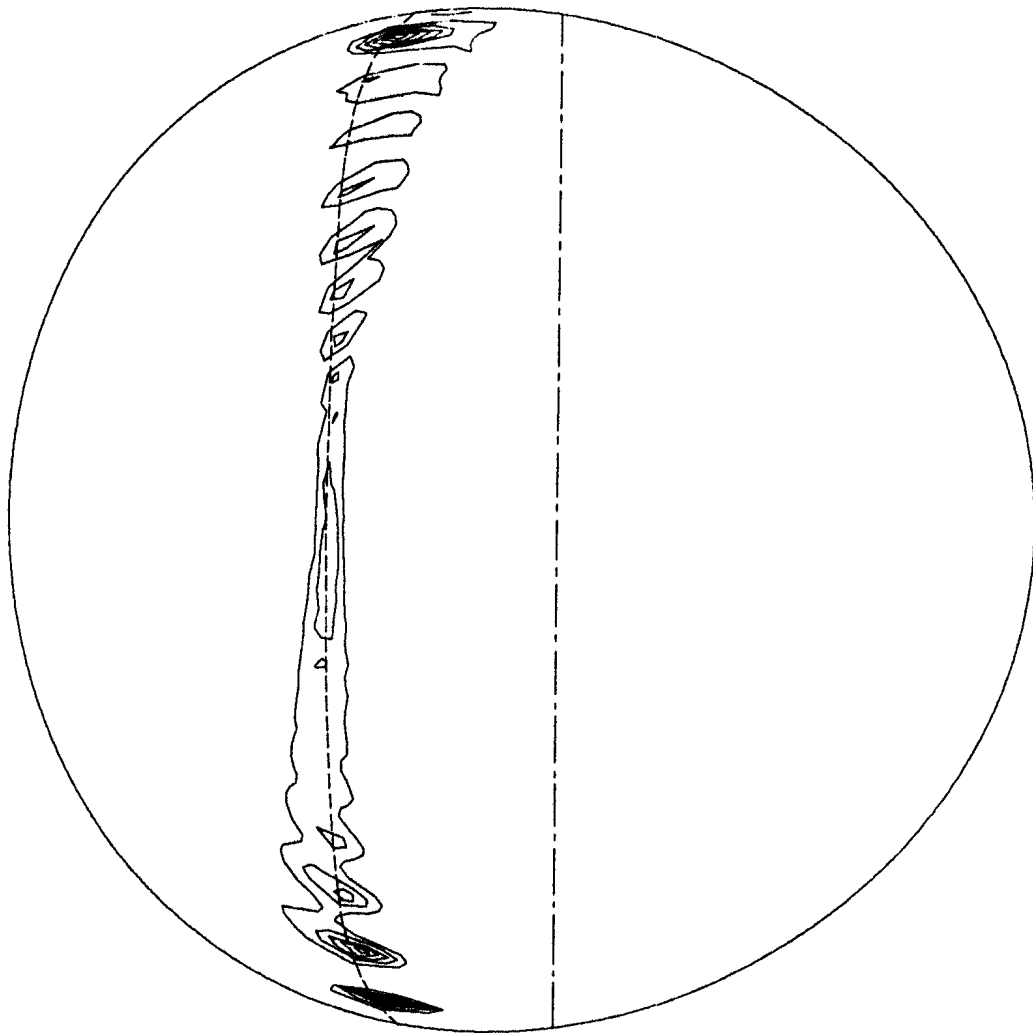


FIG. 2



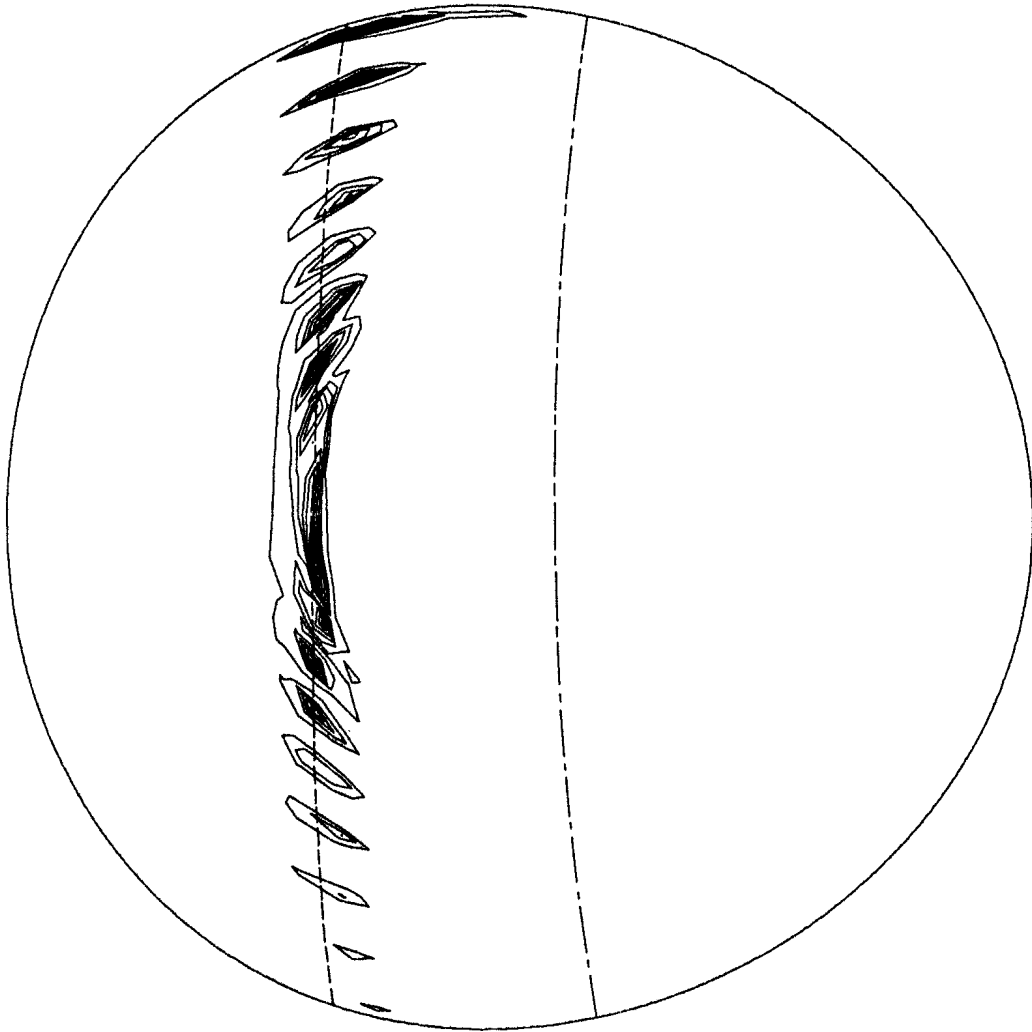
L-ION POWER ABSORPTION DENSITY
CRPP
LAUSANNE

FIG. 3



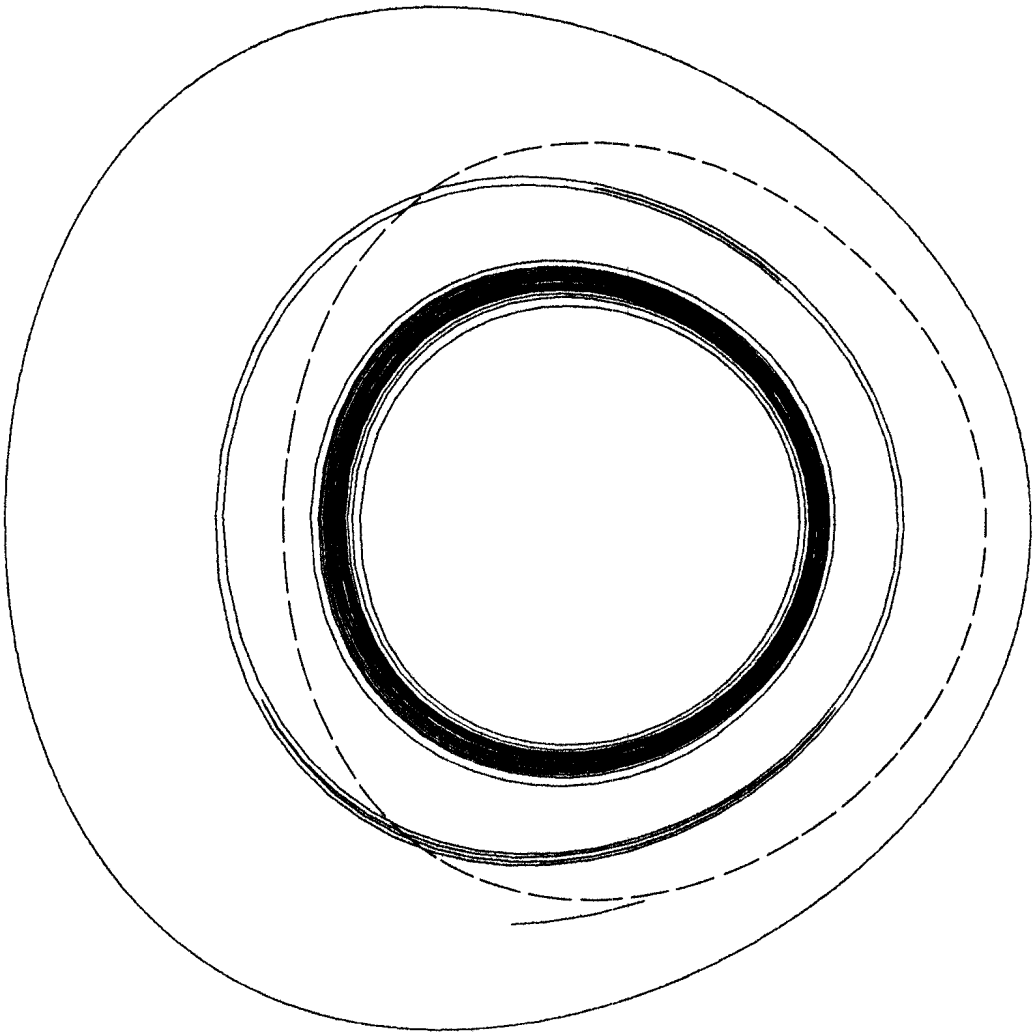
L-ION POWER ABSORPTION DENSITY
CRPP
LAUSANNE

FIG. 4



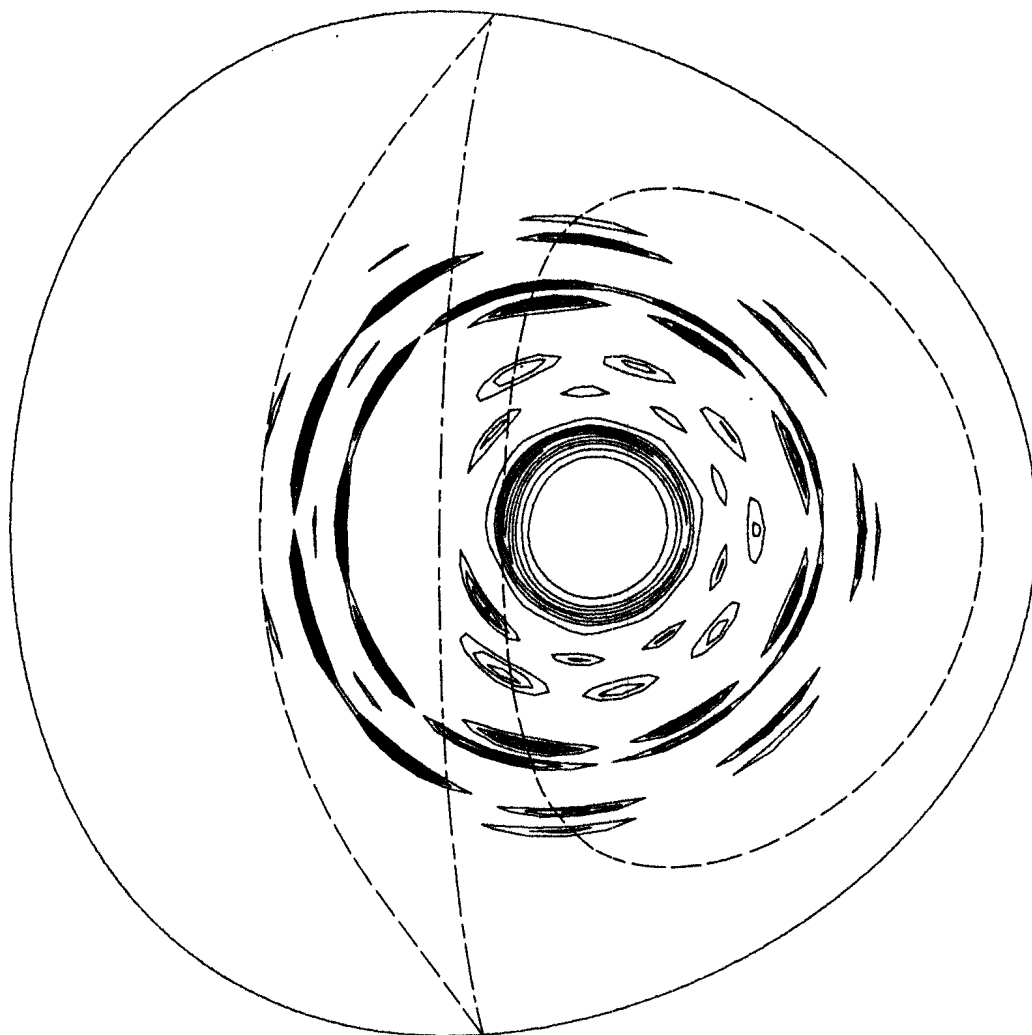
L-ION POWER ABSORPTION DENSITY
CRPP
LAUSANNE

FIG. 5



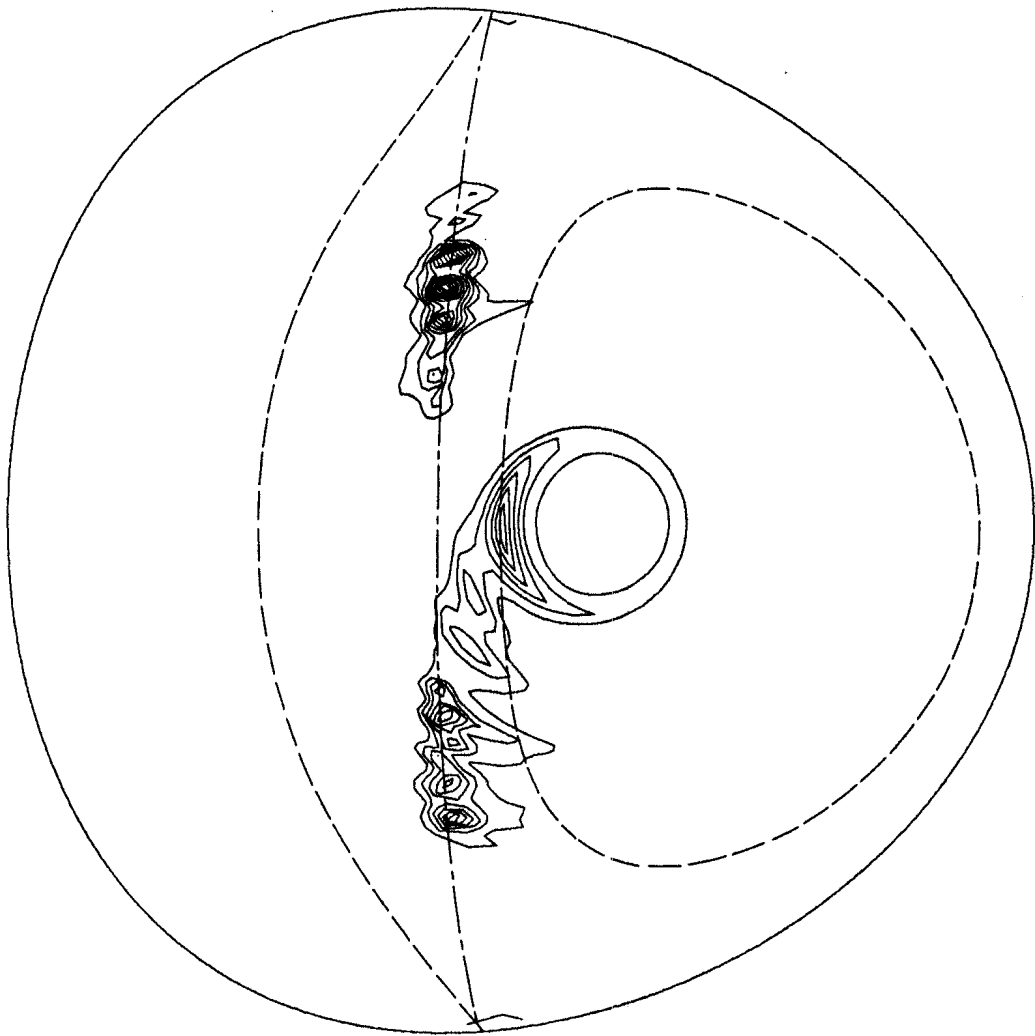
L-ION POWER ABSORPTION DENSITY
CRPP
LAUSANNE

FIG. 6A



L-ION POWER ABSORPTION DENSITY
CRPP
LAUSANNE

FIG. 6B



L-ION POWER ABSORPTION DENSITY
CRPP
LAUSANNE

FIG. 7

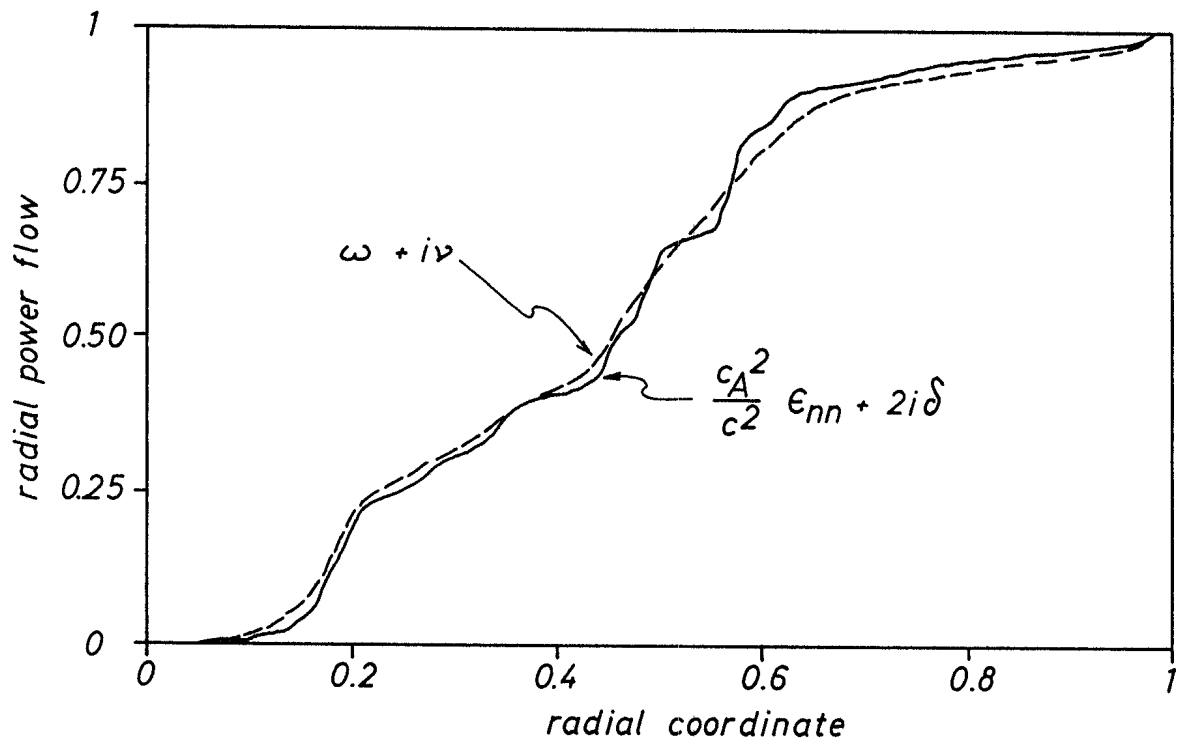


FIG. 8

